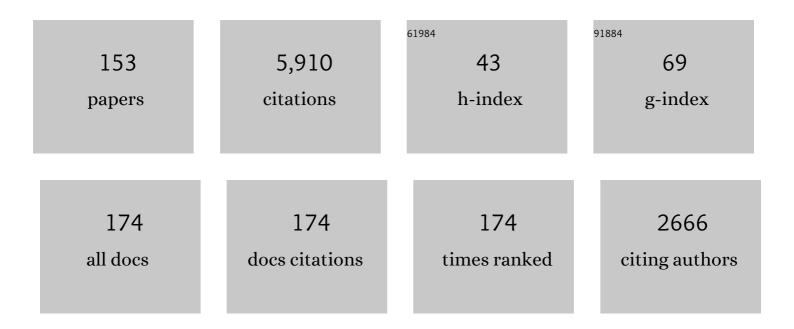
List of Publications by Year in descending order

Source: https://exaly.com/author-pdf/4618880/publications.pdf Version: 2024-02-01



#	Article	IF	CITATIONS
1	The Analyser of Space Plasmas and Energetic Atoms (ASPERA-4) for the Venus Express mission. Planetary and Space Science, 2007, 55, 1772-1792.	1.7	214
2	Solar Wind-Induced Atmospheric Erosion at Mars: First Results from ASPERA-3 on Mars Express. Science, 2004, 305, 1933-1936.	12.6	204
3	The Two Wide-angle Imaging Neutral-atom Spectrometers (TWINS) NASA Mission-of-Opportunity. Space Science Reviews, 2009, 142, 157-231.	8.1	170
4	The loss of ions from Venus through the plasma wake. Nature, 2007, 450, 650-653.	27.8	168
5	Dynamics of Saturn's Magnetosphere from MIMI During Cassini's Orbital Insertion. Science, 2005, 307, 1270-1273.	12.6	166
6	Storm time evolution of the outer radiation belt: Transport and losses. Journal of Geophysical Research, 2006, 111, .	3.3	155
7	Radiation Belt Storm Probes Ion Composition Experiment (RBSPICE). Space Science Reviews, 2013, 179, 263-308.	8.1	155
8	Recurrent energization of plasma in the midnight-to-dawn quadrant of Saturn's magnetosphere, and its relationship to auroral UV and radio emissions. Planetary and Space Science, 2009, 57, 1732-1742.	1.7	140
9	Energetic ion acceleration in Saturn's magnetotail: Substorms at Saturn?. Geophysical Research Letters, 2005, 32, .	4.0	124
10	Global imaging of O+from IMAGE/HENA. Space Science Reviews, 2003, 109, 63-75.	8.1	120
11	Plasma Acceleration Above Martian Magnetic Anomalies. Science, 2006, 311, 980-983.	12.6	111
12	Energetic ion spectral characteristics in the Saturnian magnetosphere using Cassini/MIMI measurements. Journal of Geophysical Research, 2009, 114, .	3.3	111
13	Energetic particle injections in Saturn's magnetosphere. Geophysical Research Letters, 2005, 32, n/a-n/a.	4.0	109
14	Mars Express and Venus Express multi-point observations of geoeffective solar flare events in December 2006. Planetary and Space Science, 2008, 56, 873-880.	1.7	102
15	Magnetospheric and auroral activity during the 18 April 2002 sawtooth event. Journal of Geophysical Research, 2006, 111, .	3.3	100
16	Impulsive enhancements of oxygen ions during substorms. Journal of Geophysical Research, 2006, 111, .	3.3	99
17	Energization of O ⁺ ions in the Earth's inner magnetosphere and the effects on ring current buildup: A review of previous observations and possible mechanisms. Journal of Geophysical Research: Space Physics, 2013, 118, 4441-4464.	2.4	94
18	Global ENA observations of the storm mainphase ring current: Implications for skewed electric fields in the inner magnetosphere. Geophysical Research Letters, 2002, 29, 15-1-15-3.	4.0	92

#	Article	IF	CITATIONS
19	Dynamical dataâ€based modeling of the stormâ€ŧime geomagnetic field with enhanced spatial resolution. Journal of Geophysical Research, 2008, 113, .	3.3	77
20	Global dynamics of the plasmasphere and ring current during magnetic storms. Geophysical Research Letters, 2001, 28, 1159-1162.	4.0	75
21	Multispectral simultaneous diagnosis of Saturn's aurorae throughout a planetary rotation. Journal of Geophysical Research: Space Physics, 2013, 118, 4817-4843.	2.4	74
22	lmaging two geomagnetic storms in energetic neutral atoms. Geophysical Research Letters, 2001, 28, 1151-1154.	4.0	73
23	Periodic intensity variations in global ENA images of Saturn. Geophysical Research Letters, 2005, 32, .	4.0	71
24	Parametric analysis of nightside conductance effects on inner magnetospheric dynamics for the 17 April 2002 storm. Journal of Geophysical Research, 2005, 110, .	3.3	65
25	Location of the bow shock and ion composition boundaries at Venus—initial determinations from Venus Express ASPERA-4. Planetary and Space Science, 2008, 56, 780-784.	1.7	64
26	ENA periodicities at Saturn. Geophysical Research Letters, 2008, 35, .	4.0	57
27	The science case for an orbital mission to Uranus: Exploring the origins and evolution of ice giant planets. Planetary and Space Science, 2014, 104, 122-140.	1.7	56
28	First ENA observations at Mars: ENA emissions from the martian upper atmosphere. Icarus, 2006, 182, 424-430.	2.5	53
29	Energetic neutral atom imaging by the Astrid microsatellite. Advances in Space Research, 1997, 20, 1055-1060.	2.6	51
30	First comparisons of local ion measurements in the inner magnetosphere with energetic neutral atom magnetospheric image inversions: Cluster-CIS and IMAGE-HENA observations. Journal of Geophysical Research, 2004, 109, .	3.3	51
31	IMAGE/high-energy energetic neutral atom: Global energetic neutral atom imaging of the plasma sheet and ring current during substorms. Journal of Geophysical Research, 2002, 107, SMP 21-1-SMP 21-13.	3.3	48
32	Ionospheric plasma acceleration at Mars: ASPERA-3 results. Icarus, 2006, 182, 308-319.	2.5	48
33	Ionospheric photoelectrons at Venus: Initial observations by ASPERA-4 ELS. Planetary and Space Science, 2008, 56, 802-806.	1.7	48
34	Comparative analysis of Venus and Mars magnetotails. Planetary and Space Science, 2008, 56, 812-817.	1.7	48
35	Statistical morphology of ENA emissions at Saturn. Journal of Geophysical Research, 2008, 113, .	3.3	48
36	Magnetic field dipolarization in the deep inner magnetosphere and its role in development of O ⁺ â€rich ring current. Journal of Geophysical Research, 2010, 115, .	3.3	48

#	Article	IF	CITATIONS
37	Imaging Plasma Density Structures in the Soft X-Rays Generated by Solar Wind Charge Exchange with Neutrals. Space Science Reviews, 2018, 214, 1.	8.1	47
38	Initial ion equatorial pitch angle distributions from medium and high energy neutral atom images obtained by IMAGE. Geophysical Research Letters, 2001, 28, 1155-1158.	4.0	46
39	Storm-substorm relationship: Variations of the hydrogen and oxygen energetic neutral atom intensities during storm-time substorms. Journal of Geophysical Research, 2005, 110, .	3.3	46
40	Energetic electrons injected into Saturn's neutral gas cloud. Geophysical Research Letters, 2007, 34, .	4.0	46
41	Energetic Neutral Atom Emissions from Titan Interaction with Saturn's Magnetosphere. Science, 2005, 308, 989-992.	12.6	44
42	Periodic tilting of Saturn's plasma sheet. Geophysical Research Letters, 2008, 35, .	4.0	44
43	Uranus Pathfinder: exploring the origins and evolution of Ice Giant planets. Experimental Astronomy, 2012, 33, 753-791.	3.7	44
44	Comparison of TWINS images of lowâ€altitude emission of energetic neutral atoms with DMSP precipitating ion fluxes. Journal of Geophysical Research, 2010, 115, .	3.3	43
45	First ENA observations at Mars: Subsolar ENA jet. Icarus, 2006, 182, 413-423.	2.5	42
46	Dynamics of ring current and electric fields in the inner magnetosphere during disturbed periods: CRCM–BATSâ€Râ€US coupled model. Journal of Geophysical Research, 2010, 115, .	3.3	42
47	On ionospheric trough conductance and subauroral polarization streams: Simulation results. Journal of Geophysical Research, 2008, 113, .	3.3	41
48	Anti-planetward auroral electron beams at Saturn. Nature, 2006, 439, 699-702.	27.8	40
49	Cluster observations in the inner magnetosphere during the 18 April 2002 sawtooth event: Dipolarization and injection at <i>r</i> = 4.6 <i>R</i> _{<i>E</i>} . Journal of Geophysical Research, 2007, 112, .	3.3	40
50	First ENA observations at Mars: Charge exchange ENAs produced in the magnetosheath. Icarus, 2006, 182, 431-438.	2.5	39
51	Ring current dynamics in moderate and strong storms: Comparative analysis of TWINS and IMAGE/HENA data with the Comprehensive Ring Current Model. Journal of Geophysical Research, 2010, 115, .	3.3	39
52	Evolution of lowâ€altitude and ring current ENA emissions from a moderate magnetospheric storm: Continuous and simultaneous TWINS observations. Journal of Geophysical Research, 2010, 115, .	3.3	39
53	Empirical modeling of a CIRâ€driven magnetic storm. Journal of Geophysical Research, 2010, 115, .	3.3	38
54	Energetic neutral atom imaging at low altitudes from the Swedish microsatellite Astrid: Images and spectral analysis. Journal of Geophysical Research, 1999, 104, 2367-2379.	3.3	37

#	Article	IF	CITATIONS
55	Analyzing electric field morphology through data-model comparisons of the Geospace Environment Modeling Inner Magnetosphere/Storm Assessment Challenge events. Journal of Geophysical Research, 2006, 111, .	3.3	37
56	Saturn's periodic magnetic field perturbations caused by a rotating partial ring current. Geophysical Research Letters, 2010, 37, .	4.0	37
57	Towards a Global Unified Model of Europa's Tenuous Atmosphere. Space Science Reviews, 2018, 214, 1.	8.1	36
58	Energetic neutral atom imaging at low altitudes from the Swedish microsatellite Astrid: Extraction of the equatorial ion distribution. Journal of Geophysical Research, 2001, 106, 25731-25744.	3.3	35
59	The exosphere of Titan and its interaction with the kronian magnetosphere: MIMI observations and modeling. Planetary and Space Science, 2007, 55, 165-173.	1.7	34
60	Transport of energetic electrons into Saturn's inner magnetosphere. Journal of Geophysical Research, 2010, 115, .	3.3	34
61	Statistical analysis of the energetic ion and ENA data for the Titan environment. Planetary and Space Science, 2010, 58, 1811-1822.	1.7	32
62	Rapid decay of storm time ring current due to pitch angle scattering in curved field line. Journal of Geophysical Research, 2011, 116, .	3.3	32
63	1. Transport of Mass, Momentum and Energy in Planetary Magnetodisc Regions. Space Science Reviews, 2015, 187, 229-299.	8.1	32
64	Contribution of charge exchange loss to the storm time ring current decay: IMAGE/HENA observations. Journal of Geophysical Research, 2006, 111, .	3.3	30
65	Understanding the global evolution of Saturn's ring current. Geophysical Research Letters, 2008, 35, .	4.0	30
66	The extended Saturnian neutral cloud as revealed by global ENA simulations using Cassini/MIMI measurements. Journal of Geophysical Research: Space Physics, 2013, 118, 3027-3041.	2.4	30
67	Energetic neutral atom imaging at low altitudes from the Swedish microsatellite Astrid: Observations at low (≇0 keV) energies. Journal of Geophysical Research, 2001, 106, 24663-24674.	3.3	29
68	Tail-dominated storm main phase: 31 March 2001. Journal of Geophysical Research, 2003, 108, .	3.3	29
69	Storm-time convection electric field in the near-Earth plasma sheet. Journal of Geophysical Research, 2005, 110, .	3.3	29
70	Auroral Plasma Acceleration Above Martian Magnetic Anomalies. Space Science Reviews, 2007, 126, 333-354.	8.1	28
71	Asymmetries in Saturn's radiation belts. Journal of Geophysical Research, 2010, 115, .	3.3	28
72	The distribution of Titan's high-altitude (out to â^¼50,000km) exosphere from energetic neutral atom (ENA) measurements by Cassini/INCA. Planetary and Space Science, 2012, 60, 107-114.	1.7	28

#	Article	IF	CITATIONS
73	First ENA observations at Mars: Solar-wind ENAs on the nightside. Icarus, 2006, 182, 439-447.	2.5	27
74	A radiation belt of energetic protons located between Saturn and its rings. Science, 2018, 362, .	12.6	27
75	IBEX Backgrounds and Signal-to-Noise Ratio. Space Science Reviews, 2009, 146, 173-206.	8.1	26
76	Properties of planetward ion flows in Venus' magnetotail. Icarus, 2016, 274, 73-82.	2.5	25
77	Relationship between Region 2 field-aligned current and the ring current: Model results. Journal of Geophysical Research, 2006, 111, .	3.3	24
78	Massâ€dependent evolution of energetic neutral atoms energy spectra during storm time substorms: Implication for O ⁺ nonadiabatic acceleration. Journal of Geophysical Research, 2010, 115, .	3.3	24
79	Ion acceleration processes in the Hermean and terrestrial magnetospheres. Advances in Space Research, 1997, 19, 1593-1607.	2.6	22
80	Energetic Neutral Atoms (ENA) at Mars: Properties of the hydrogen atoms produced upstream of the martian bow shock and implications for ENA sounding technique around non-magnetized planets. Icarus, 2006, 182, 448-463.	2.5	22
81	The Venusian induced magnetosphere: A case study of plasma and magnetic field measurements on the Venus Express mission. Planetary and Space Science, 2008, 56, 796-801.	1.7	22
82	Energetic neutral atom imaging of Mercury's magnetosphere 2. Distribution of energetic charged particles in a compact magnetosphere. Planetary and Space Science, 2001, 49, 1677-1684.	1.7	21
83	Bastille Day storm: Global response of the terrestrial ring current. Solar Physics, 2001, 204, 377-386.	2.5	21
84	Statistical characteristics of hydrogen and oxygen ENA emission from the storm-time ring current. Journal of Geophysical Research, 2006, 111, .	3.3	21
85	IMF Direction Derived from Cycloid-Like Ion Distributions Observed by Mars Express. Space Science Reviews, 2007, 126, 239-266.	8.1	21
86	Rice Convection Model simulation of the 18 April 2002 sawtooth event and evidence for interchange instability. Journal of Geophysical Research, 2008, 113, .	3.3	21
87	Evolution of mass density and O+ concentration at geostationary orbit during storm and quiet events. Journal of Geophysical Research: Space Physics, 2014, 119, 6417-6431.	2.4	21
88	The Role and Contributions of Energetic Neutral Atom (ENA) Imaging in Magnetospheric Substorm Research. Space Science Reviews, 2003, 109, 155-182.	8.1	20
89	Nightside thermospheric FUV emissions due to energetic neutral atom precipitation during magnetic superstorms. Journal of Geophysical Research, 2006, 111, .	3.3	20
90	Modeling global O+ substorm injection using analytic magnetic field model. Journal of Geophysical Research, 2006, 111, .	3.3	20

#	Article	IF	CITATIONS
91	Source location of the wedge-like dispersed ring current in the morning sector during a substorm. Journal of Geophysical Research, 2006, 111, .	3.3	20
92	First observation of energetic neutral atoms in the Venus environment. Planetary and Space Science, 2008, 56, 807-811.	1.7	19
93	Track analysis of energetic neutral atom blobs at Saturn. Journal of Geophysical Research, 2008, 113, .	3.3	19
94	Interstellar Probe: Humanity's exploration of the Galaxy Begins. Acta Astronautica, 2022, 199, 364-373.	3.2	19
95	ENA detection in the dayside of Mars: ASPERA-3 NPD statistical study. Planetary and Space Science, 2008, 56, 840-845.	1.7	18
96	The lower exosphere of Titan: Energetic neutral atoms absorption and imaging. Journal of Geophysical Research, 2008, 113, .	3.3	18
97	The ion population of the magnetotail during the 17 April 2002 magnetic storm: Large-scale kinetic simulations and IMACE/HENA observations. Journal of Geophysical Research, 2011, 116, .	3.3	18
98	Energetic neutral atom imaging of Mercury's magnetosphere 3. Simulated images and instrument requirements. Planetary and Space Science, 2001, 49, 1685-1692.	1.7	17
99	Energetic neutral atom response to solar wind dynamic pressure enhancements. Journal of Geophysical Research, 2007, 112, .	3.3	17
100	A method for estimating the ring current structure and the electric potential distribution using energetic neutral atom data assimilation. Journal of Geophysical Research, 2008, 113, .	3.3	17
101	Ground and satellite observations of lowâ€ŀatitude red auroras at the initial phase of magnetic storms. Journal of Geophysical Research: Space Physics, 2013, 118, 256-270.	2.4	17
102	Interstellar probe $\hat{a} \in $ Destination: Universe!. Acta Astronautica, 2022, 196, 13-28.	3.2	17
103	Inductive electric fields in the inner magnetosphere during geomagnetically active periods. Journal of Geophysical Research, 2010, 115, .	3.3	16
104	Magnetospheric Studies: A Requirement for Addressing Interdisciplinary Mysteries in the Ice Giant Systems. Space Science Reviews, 2020, 216, 1.	8.1	16
105	Proton temperatures in the ring current from ENA images and in situ measurements. Geophysical Research Letters, 2005, 32, .	4.0	15
106	The "Puck―energetic charged particle detector: Design, heritage, and advancements. Journal of Geophysical Research: Space Physics, 2016, 121, 7900-7913.	2.4	15
107	Energetic particle imaging: The evolution of techniques in imaging highâ€energy neutral atom emissions. Journal of Geophysical Research: Space Physics, 2016, 121, 8804-8820.	2.4	15
108	Small-scale structure in the stormtime ring current. Geophysical Monograph Series, 2005, , 167-177.	0.1	14

#	Article	IF	CITATIONS
109	Energetic neutral atom (ENA) and charged particle periodicities in Saturn's magnetosphere. Advances in Space Research, 2009, 44, 483-493.	2.6	14
110	Moderate geomagnetic storm (21–22 January 2005) triggered by an outstanding coronal mass ejection viewed via energetic neutral atoms. Journal of Geophysical Research, 2010, 115, .	3.3	14
111	Evolution of ring current ion energy spectra during the storm recovery phase: Implication for dominant ion loss processes. Journal of Geophysical Research, 2011, 116, .	3.3	14
112	Storm-time enhancement of mid-latitude ultraviolet emissions due to energetic neutral atom precipitation. Geophysical Research Letters, 2005, 32, .	4.0	13
113	Soft Xâ€ray and ENA Imaging of the Earth's Dayside Magnetosphere. Journal of Geophysical Research: Space Physics, 2021, 126, e2020JA028816.	2.4	13
114	Storm-substorm relationships during the 4 October, 2000 storm. IMAGE Global ENA imaging results. Geophysical Monograph Series, 2003, , 103-118.	0.1	12
115	Periodic Narrowband Radio Wave Emissions and Inward Plasma Transport at Saturn's Magnetosphere. Astronomical Journal, 2020, 159, 249.	4.7	12
116	An overview of the scientific objectives and technical configuration of the NeUtral Atom Detector Unit (NUADU) for the Chinese Double Star Mission. Planetary and Space Science, 2005, 53, 335-348.	1.7	11
117	Empirical Modeling of Extreme Events: Storm-Time Geomagnetic Field, Electric Current, and Pressure Distributions. , 2018, , 259-279.		11
118	Radiation Belt Storm Probes Ion Composition Experiment (RBSPICE). , 2013, , 263-308.		11
119	The NUADU experiment on TC-2 and the first Energetic Neutral Atom (ENA) images recorded by this instrument. Annales Geophysicae, 2005, 23, 2825-2849.	1.6	10
120	Observations of energetic neutral oxygen by IMAGE/HENA and Geotail/EPIC. Geophysical Research Letters, 2005, 32, .	4.0	10
121	Iterative inversion of global magnetospheric ion distributions using energetic neutral atom (ENA) images recorded by the NUADU/TC2 instrument. Annales Geophysicae, 2008, 26, 1641-1652.	1.6	10
122	String-fluid transition in systems with aligned anisotropic interactions. Journal of Chemical Physics, 2010, 132, 234709.	3.0	10
123	Low-energy energetic neutral atom imaging of Io plasma and neutral tori. Planetary and Space Science, 2015, 108, 41-53.	1.7	10
124	Decrease in SYM-H during a storm main phase without evidence of a ring current injection. Journal of Atmospheric and Solar-Terrestrial Physics, 2015, 134, 118-129.	1.6	10
125	Reconstruction of Extreme Geomagnetic Storms: Breaking the Data Paucity Curse. Space Weather, 2020, 18, e2020SW002561.	3.7	10
126	Modeling the ring current response to a sawtooth oscillation event. Journal of Atmospheric and Solar-Terrestrial Physics, 2007, 69, 67-76.	1.6	9

#	Article	IF	CITATIONS
127	The Linkage between the Ring Current and the Ionosphere System. Geophysical Monograph Series, 0, , 135-143.	0.1	9
128	Venusian bow shock as seen by the ASPERAâ€4 ion instrument on Venus Express. Journal of Geophysical Research, 2010, 115, .	3.3	9
129	Comparisons between ion distributions retrieved from ENA images of the ring current and contemporaneous, multipoint ion measurements recorded in situ during the major magnetic storm of 15 May 2005. Journal of Geophysical Research, 2010, 115, .	3.3	9
130	ENA periodicities and their phase relations to SKR emissions at Saturn. Geophysical Research Letters, 2011, 38, n/a-n/a.	4.0	9
131	HELIOSPHERIC ENERGETIC NEUTRAL HYDROGEN MEASURED WITH ASPERA-3 AND ASPERA-4. Astrophysical Journal, 2013, 775, 24.	4.5	8
132	Estimation of temporal evolution of the helium plasmasphere based on a sequence of IMAGE/EUV images. Journal of Geophysical Research: Space Physics, 2014, 119, 3708-3723.	2.4	8
133	Statistical analysis of the observations of the MEX/ASPERA-3 NPI in the shadow. Planetary and Space Science, 2009, 57, 1000-1007.	1.7	7
134	Titan's exosphere and its interaction with Saturn's magnetosphere. Philosophical Transactions Series A, Mathematical, Physical, and Engineering Sciences, 2009, 367, 743-752.	3.4	7
135	Interstellar Probe: A Practical Mission to Escape the Heliosphere. , 2021, , .		7
136	On the relation between electric fields in the inner magnetosphere, ring current, auroral conductance, and plasmapause motion. Geophysical Monograph Series, 2005, , 159-166.	0.1	6
137	Oxygen in the ring current during major storms. Advances in Space Research, 2005, 36, 1758-1761.	2.6	6
138	Local time dependences of oxygen ENA periodicities at Saturn. Journal of Geophysical Research: Space Physics, 2014, 119, 6577-6586.	2.4	6
139	Estimation of the helium ion density distribution in the plasmasphere based on a single IMAGE/EUV image. Journal of Geophysical Research: Space Physics, 2014, 119, 3724-3740.	2.4	6
140	The Lowâ€Energy Neutral Imager (LENI). Journal of Geophysical Research: Space Physics, 2016, 121, 8228-8236.	2.4	6
141	Convection electric field in the near-Earth tail during the super magnetic storm of November 20–21, 2003. Geophysical Research Letters, 2006, 33, .	4.0	5
142	Energetic, â^1⁄45–90 keV neutral atom imaging of a weak substorm with STEREO/STE. Geophysical Research Letters, 2010, 37, .	4.0	4
143	Dynamic Challenges of Long Flexible Booms on a Spinning Outer Heliospheric Spacecraft. , 2021, , .		4
144	Controlling factors of Region 2 field-aligned current and its relationship to the ring current: Model results. Advances in Space Research, 2008, 41, 1234-1242.	2.6	3

#	Article	IF	CITATIONS
145	A Residual Source of Energetic Neutral Atoms Across the Sky Obtained by the Neutral Particle Detector on board Venus Express. , 2009, , .		3
146	Enabling a Near-Term Interstellar Probe with the Space Launch System. , 2019, , .		3
147	Electron pitch angle variations recorded at the high magnetic latitude boundary layer by the NUADU instrument on the TC-2 spacecraft. Annales Geophysicae, 2005, 23, 2953-2959.	1.6	1
148	Using measurements of Energetic Neutral Atoms from low Earth orbit to infer global magnetospheric ion distributions. Journal of Geophysical Research, 2008, 113, .	3.3	1
149	Magnetic field depression at the Earth's surface during energetic neutral atom emission fade-out in the inner magnetosphere. Journal of Geophysical Research, 2011, 116, n/a-n/a.	3.3	1
150	The Storm-Time Injection of Ions into the Inner Magnetosphere: Large-Scale Kinetic Simulations and IMAGEâ^•HENA Observations. AIP Conference Proceedings, 2011, , .	0.4	1
151	Phase transitions in 2D plasma crystals driven by tunable interactions. , 2012, , .		0
152	Transport of Mass, Momentum and Energy in Planetary Magnetodisc Regions. Space Sciences Series of ISSI, 2016, , 229-299.	0.0	0
153	Energetic neutral atom imaging of the terrestrial global magnetosphere. , 2022, , 23-58.		0